

<https://doi.org/10.1038/s42004-024-01140-3>

Synergetic binary organocatalyzed ring opening polymerization for the precision synthesis of polysiloxanes

Check for updates

Hiroshi Okamoto¹, Atsushi Sogabe¹ & Satoshi Honda^{1,2} ✉

Organocatalytic ring-opening polymerization (ROP) is a versatile method for synthesizing well-defined polymers with controlled molecular weights, dispersities, and nonlinear macromolecular architectures. Despite spectacular advances in organocatalytic ROP, precision synthesis of polysiloxanes remains challenging due to the mismatch in polarity between highly polar initiators and nonpolar monomers and polymers and the difficulty in suppressing the formation of scrambling products via transesterification reactions during ROP of cyclic siloxanes. Here, we describe a binary organocatalytic ROP (BOROP) of hexamethylcyclotrisiloxane (D3) employing organic bases as catalysts and (thio)ureas as cocatalysts. The BOROP of D3 using triazabicyclodecene (TBD) and (thio)ureas generates polydimethylsiloxanes (PDMSs) with narrow dispersity ($M_w/M_n < 1.1$). Despite the similar basicities of TBD and 1,8-bis(tetramethylguanidino)naphthalene (TMGN), which is known as a proton sponge, a unitary organocatalytic system using TMGN was inactive for the ROP of D3. When the TMGN was paired with acidic urea, the BOROP of D3 yielded PDMSs with narrow dispersity ($M_w/M_n < 1.1$). Data suggest that the synergetic effect of TMGN and urea results in an unprecedented activation–deactivation equilibrium between dormant and propagating species. The benefits of the present BOROP system are demonstrated by the formation of PDMS elastomers with more uniform network structures that are highly stretchy and have excellent mechanical properties.

Ring-opening polymerization (ROP) is an important class of methodologies for synthesizing polymers with controlled molecular weights (MWs) and narrow dispersities (D_s)¹. Encouraged by the first report of organocatalytic ROP utilizing 4-dimethylaminopyridine (DMAP) by Hedrick et al. in 2001², herculean efforts over the years in this area have led to the development of a great number of organocatalysts such as amidine and guanidine bases^{3,4}, *N*-heterocyclic carbenes (NHCs)^{5,6}, phosphazenes^{7,8}, and urea anions⁹. These catalysts have been shown to exhibit excellent activity, selectivity, and compatibility with various monomers including epoxides, lactones, and carbonates, to mention a few, in addition to often being considered less toxic than metal-based catalysts^{10–12}.

Polysiloxanes are industrially important materials that cannot be replaced by carbon-based polymers due to their unique properties such as high thermal stability, low surface energy, and excellent biocompatibility¹³. Historically, polysiloxanes have been synthesized by equilibrium polymerization using strong acids or catalyst-free ROP of cyclic siloxanes^{14,15}. As polysiloxanes synthesized by equilibrium polymerization have broad

dispersity ($M_w/M_n = D$), synthesizing polysiloxanes by ROP of cyclic siloxanes is important when expected applications require controlled MW with narrow D ^{16,17}. In particular, the use of organic catalysts in the ROP of cyclic siloxanes is attractive as reported by Hedrick, Waymouth, and coworkers^{18,19}. Unlike other organic catalysts, ROP of 2,2,5,5-tetramethyl-1-oxa-2,5-disilacyclopentane (TMOSC) using 1,5,7-triazabicyclo[4.4.0]dec-5-ene (TBD) after full conversion of monomers did not show a broadening in dispersity¹⁸. They also reported that organocatalytic ROP of cyclic siloxanes initiated from silanols¹⁸ can avoid the inclusion of labile Si-O-C linkages, or silylether to the resulting polysiloxane. Inspired by these prominent studies, we synthesized star-shaped polydimethylsiloxanes (PDMSs) with controlled MWs and D_s upon organocatalytic ROP of hexamethylcyclotrisiloxane (D3) initiated from trifunctional silanols²⁰. Although a mixture of TBD and trifunctional silanol showed poor solubility in solvents for polymerization due to the mismatch of the highly polar nature of initiating system with nonpolar monomers and polymers, an initiating system using urea anions overcomes this problem. In fact, ROP using urea anions affords

¹MIRAI Technology Institute, Shiseido Co. Ltd, 1-2-11 Takashima, Nishi-ku, Yokohama, Kanagawa 220-0011, Japan. ²Graduate School of Arts and Sciences, The University of Tokyo, 3-8-1 Komaba, Meguro-ku, Tokyo 153-8902, Japan. ✉ e-mail: c-honda@mail.ecc.u-tokyo.ac.jp

polymers with a narrow \bar{D} when the conversion of D3 is low. However, with urea anions, the ROP reaches equilibrium when the conversion of D3 exceeds approximately 50%, and the \bar{D} of the resulting PDMS in the mixture broadens²⁰. Hence, in addition to solubilizing the initiating system, developing an efficient catalyst system that can avoid equilibrium polymerization with the ROP of siloxanes²¹ remains a crucial challenge.

Herein, we report the binary organocatalytic ROP (BOROP) of D3 using organic bases as catalysts and (thio)ureas as cocatalysts. The synergetic use of TBD and (thio)urea for the ROP of D3 enables both the solubilization of multifunctional silanols in THF and the production of PDMS with a narrow \bar{D} until the monomer conversion reaches approximately 90%. Moreover, we investigated the applicability of proton sponges for the ROP of D3. While a unitary organocatalytic system using proton sponges was inactive, ROP of D3 proceeded with the synergetic use of 1,8-bis(trimethylguanidino)naphthalene (TMGN) and urea. In the cocatalytic system with TBD and urea, ROP is accelerated with less acidic urea. Despite the similar basicities of TBD and TMGN, ROP was accelerated by the addition of more acidic urea. Mechanistically, this suggests that the BOROP system using TMGN is in activation–deactivation equilibrium between dormant and propagating species, similar to what has been reported for living radical polymerization. The advantage of the present BOROP system was finally confirmed by the excellent mechanical properties of highly stretchy elastomeric PDMS formed from three-armed star-shaped PDMSs. The developed BOROP would be highly beneficial for the precision synthesis of polysiloxanes and enables facile access to those with branched macromolecular architectures with narrow \bar{D} .

Results and discussion

ROP of D3 with a unitary organocatalytic system

We first surveyed the basicity of a series of organic bases. The pK_a values of the conjugate acids of these bases (pK_{BH^+}) in MeCN indicate similar catalytic activities between DMAP ($pK_{BH^+} = 17.95$)²² and 1,8-bis(dimethylamino)naphthalene (DMAN) ($pK_{BH^+} = 18.18$)²³ and between TBD ($pK_{BH^+} = 26.03$)²² and TMGN ($pK_{BH^+} = 25.10$)²³ (Fig. 1). The ROP of D3 in THF ([D3] = 2.4 M) initiated from trifunctional silanol (I_3) (Fig. 2a) with these organic bases readily revealed that less basic DMAP and DMAN, which are known as a proton sponge, are inactive under the polymerization conditions tested (Table 1, entries 1 and 2). Similar to the pioneering study reported by Waymouth, Hedrick, and coworkers¹⁸, the ROP of D3 with strongly basic TBD proceeded, and the conversion reached 92% with a polymerization time of 120 min (Table 1, entry 3). Plots of monomer conversion against time determined using size exclusion chromatography (SEC) showed a monotonic increase in conversion, whereas \bar{D} apparently broadened after 60 min (Fig. 2b). While a previous study on the ROP of TMOsc indicated that TBD could prevent the formation of scrambling products via transesterification reactions¹⁹, in the case of D3, the considerably smaller M_n than that calculated from conversion ($M_{n,theo}$) and the broadening of \bar{D} at higher conversions suggest the formation of oligomers

and scrambling products (Fig. 2c). Considering that the pK_{BH^+} values of TBD and TMGN are comparable (Fig. 1), in terms of basicity, the ROP of D3 using TMGN as an organocatalyst should proceed. However, in prior literature, the organocatalytic ROP of octamethylcyclotetrasiloxane using TMGN was performed at 65 °C, suggesting difficulty in controlling ROP with TMGN²⁴. In fact, when ROP of D3 was attempted with TMGN, no monomer consumption was observed at 25 °C (Table 1, entry 4). This suggests that basicity is not the only factor affecting catalytic activity in the ROP of D3, and the bifunctionality of TBD²⁵, characterized by its dual action as both a hydrogen-bonding donor and acceptor, is probably responsible for its reactivity. Compared to TBD, TMGN is more sterically hindered; thus, the difference in the steric configuration of the basic reactive center may be responsible for the unitary polymerizability.

ROP of D3 with binary organocatalytic system

To examine the effect of cocatalysts on the ROP of D3 and to test its generality, we screened a series of ureas to be paired with TBD (Fig. 3a). We first monitored the interactions among I_3 , TBD, and U(Cy) in THF based on deuterated solvent-free benchtop ¹H NMR (80 MHz) spectrometry. While signals that should appear at 1–4 ppm in the ¹H NMR spectrum overlap with THF-derived signals, the signals appearing in the spectrum of I_3 (Supplementary Fig. 1a, marked a, b, and c) corresponded to those appearing in the separately measured ¹H NMR (500 MHz) spectrum (Supplementary ¹H NMR) and U(Cy) (Supplementary Fig. 1b, marked Ph_U), which corresponded to their reported values and that appeared in the spectrum of their mixture but remained unchanged (Supplementary Fig. 1c). When TBD was added to the THF mixture of I_3 , the resulting mixture became turbid due to the insolubility of the silanol-derived ionic species in THF. The ¹H NMR spectrum of the soluble fraction showed the disappearance of the signal derived from silanol, and the signal derived from dimethyl protons at 0.23 ppm broadened and split into two signals (marked b), also indicating its poor solubility in THF. (Supplementary Fig. 1d). Furthermore, the signal derived from the benzene ring significantly broadened and its intensity decreased. This decrease in the mobility of protons suggested that the components thought to be dissolved in THF might aggregate. In contrast, while the addition of U(Cy) to the mixture of I_3 and TBD significantly increased the intensity of the signal derived from the benzene ring of I_3 (marked a), that derived from silanol was still absent (Supplementary Fig. 1e). A more noticeable change is that the split and broadened signals derived from dimethyl groups become one narrowed signal. In addition to the fact that the addition of U(Cy) apparently solubilized the mixture of I_3 and TBD, these results also suggest a rapid and reversible exchange reaction between the silanols and TBD/U(Cy). The interactions among I_3 , TBD, and U(Cy) were further examined based on infrared (IR) spectroscopy. While the IR spectra of I_3 and U(Cy) showed broad absorptions derived from O–H (3270 cm⁻¹) and N–H (3320 cm⁻¹) stretching vibrations (Supplementary Fig. 2a, b), respectively, mixing I_3 , TBD, and U(Cy) resulted in significant broadening of the absorption at the

Fig. 1 | Organocatalysts and their pK_a s. Chemical structures of DMAP, DMAN, TBD, and TMGN and their reported pK_a s in MeCN.

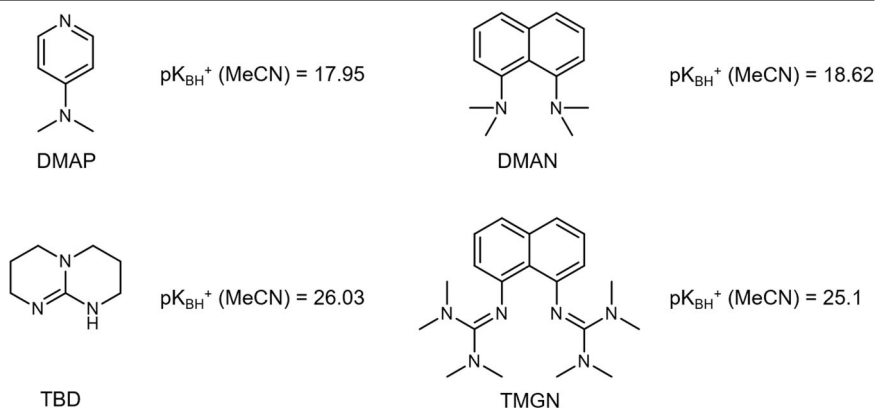
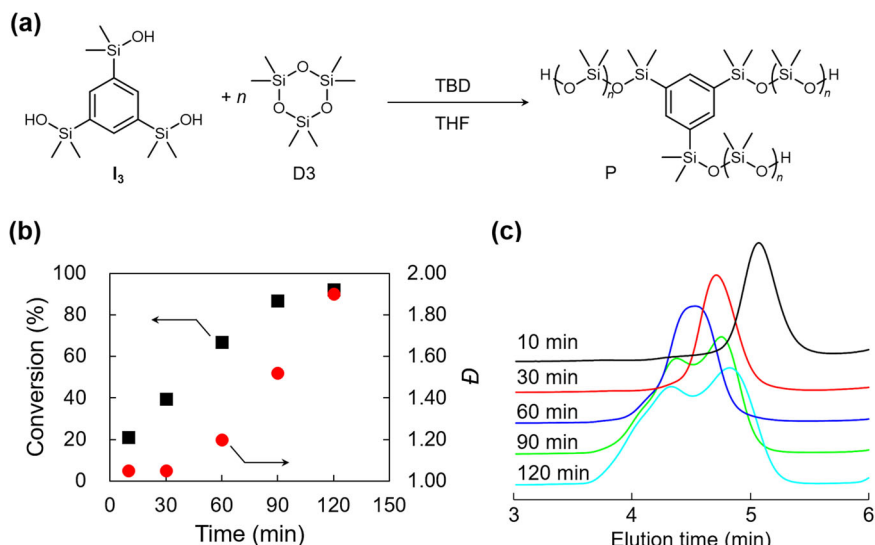


Fig. 2 | Unitary organocatalytic ROP for the synthesis of star-shaped PDMSs. **a** ROP of D3 with TBD initiated from I₃. **b** Plots of conversion and \bar{D} against time. **c** SEC traces of the products after a series of polymerization time (10, 30, 60, 90, 120 min). Source data for Fig. 2b is available (Supplementary Data 1).



relevant wavelengths (2000–3500 cm^{-1}). This suggests the presence of various types of H-bonding in the mixture and that the H-bonding nature of U(Cy) contributes to the solubilization of I₃ in the reaction mixture.

Having confirmed the effective formation of H-bonds between the silanol I₃ and TBD/U(Cy), we tested a total of 8 entries of the binary organocatalytic ROP (BOROP) of D3 under different conditions to obtain star-shaped PDMSs with narrow \bar{D} , and the results of the screening are presented in Table 2. Since TBD should extract a proton from urea in the reaction system, the reactivity of BOROP should be of the same order as the reactivity of the urea anion. With that, we started from the use of U(Cy) as a cocatalyst, which has been reported to produce the most reactive urea anion, and readily recognized that the \bar{D} of the product with monomer conversion similar to that of the unitary system (Table 1, entry 3) ($M_n = 15900$, $\bar{D} = 1.90$) was markedly narrowed (Table 2, entry 1) ($M_n = 35500$, $\bar{D} = 1.27$). A decrease in the amount of TBD further narrowed \bar{D} ($M_n = 23400$, $\bar{D} = 1.16$), and a decrease in the amount of U(Cy) resulted in the broadening of \bar{D} ($M_n = 24700$, $\bar{D} = 1.42$). These results directly demonstrated the role of urea in narrowing \bar{D} . Next, the effect of the number of CF₃ groups on BOROP was examined. As expected, the increase in the number of CF₃ groups slowed the polymerization (Table 2, entries 4–6). However, it was more interesting that \bar{D} became noticeably narrower as CF₃ increased. Remarkably, the \bar{D} of the PDMS in the polymerization mixture was less than 1.1 even when the monomer conversion reached 99% (Table 2, entry 6). The use of a more acidic TU also afforded PDMS with a narrow \bar{D} but required significantly longer reaction times (Table 2, entries 7 and 8). From these results, the synergistic use of TBD and U(4CF₃) optimizes the BOROP of D3.

Table 1 | ROP of D3 initiated from I₃ with a series of organic bases^a

Entry	Cat.	Time (min)	Conv. (%) ^b	M_n^c	\bar{D}^d
1	DMAP	120	0	N.D.	N.D.
2	DMAN	120	0	N.D.	N.D.
3	TBD	120	92	15,900 (27,600)	1.90
4	TMGN	120	0	N.D.	N.D.

^aThe polymerizations were performed at 25 °C. [I₃]₀ : [Cat.]₀ : [D3]₀ = 1:1.5:135. [I₃]₀ = 0.018 M, [D3]₀ = 2.14 M.

^bConversion determined by ¹H NMR.

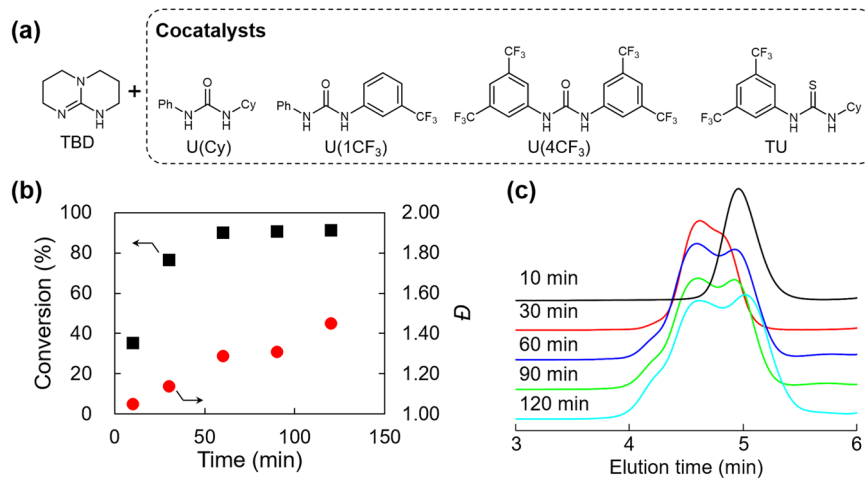
^cNumber average molecular weight, determined by SEC with RI detector. The number in the parenthesis represents molecular weight calculated from conversion.

^dDispersity ($\bar{D} = M_w/M_n$), determined by SEC. SEC measurements were performed after terminating with benzoic acid.

BOROP of D3 in activation–deactivation equilibrium between dormant and propagating species

Having optimized the BOROP conditions, we next screened organocatalysts (Fig. 1) to be paired with U(4CF₃). While less basic DMAP and DMAN were again inactive even in the presence of U(4CF₃) (Table 3, entries 1 and 2), interestingly, the BOROP of D3 with the synergistic use of TMGN and U(4CF₃) produced PDMSs with narrow \bar{D} (Table 3, entries 3 and 4). The plots of conversion against time showed exceptional linearity (Fig. 4a), and \bar{D} remained narrow even with a polymerization time of 360 min. In the case of the TBD/urea catalytic system, BOROP of D3 should proceed via neutral and imidate-mediated H-bonding mechanisms as reported previously (Fig. 4c)²⁶. However, considering that the unitary catalytic system using TMGN was inactive, activation–deactivation equilibrium, similar to that observed for living radical polymerization, such as atom transfer radical polymerization (ATRP)²⁷, can be proposed for the present synergistic BOROP system using TMGN and U(4CF₃) (Fig. 4d). Thus, when protons derived from silanols are abstracted by TMGN, the formed complex cannot attack the monomer due to the steric hindrance of the methyl groups surrounding the TMGN, as recognized in the unitary ROP system (Table 1, entry 4). On the other hand, if the abstraction of protons from U(4CF₃) is in equilibrium, the growing species can attack the monomer (Fig. 4d). Given that the pK_a of I₃ can be approximately between that of Et₃SiOH (pK_a = 13.63) and that of Ph₃SiOH (pK_a = 16.57–16.63)^{28,29}, and that the reported pK_a of U(4CF₃) is 13.8³⁰, it is reasonable to assume this equilibrium. With this activation–deactivation equilibrium between dormant and propagating species, BOROP with less acidic U(Cy) (pK_a = 22.8 (25.1))³¹ should not proceed because no proton abstraction could occur. This hypothesis was readily supported by the inactivity of the TMGN/U(Cy) cocatalytic system (Table 3, entry 5). The urea anion formed from less acidic urea is more active in the conventional ROP (Fig. 4c), following which the activation–inactivation process (Fig. 4d) mechanistically reverses the relationship between the acidity of urea and the polymerization rate, despite TBD (pK_{BH}⁺ = 26.03) and TMGN (pK_{BH}⁺ = 25.10) having similar basicities (Fig. 1). In the present case, the moderate acidity of U(4CF₃) would push the equilibrium to the left-hand side (Fig. 4d), thus resulting in slower polymerization than in the TBD/U(4CF₃) cocatalytic system. The plausibility of this hypothesis was further examined based on IR spectroscopy. First, the proton abstraction from I₃ by TMGN was supported by the comparison of IR spectra among I₃ (Supplementary Fig. 2a), TMGN (Supplementary Fig. 3a), and their mixture (Supplementary Fig. 3b) by the disappearance of absorption derived from the O–H stretching vibration (3270 cm^{-1}) visible for I₃ from their mixture. On the other hand, a comparison of the IR spectra of TMGN (Supplementary Fig. 3a), U(4CF₃) (Supplementary Fig. 3c), and

Fig. 3 | Binary organocatalytic ROP for the synthesis of star-shaped PDMSs. **a** Chemical structures of TBD and cocatalysts. **b** Plots of conversion and \bar{D} against time and **(c)** SEC traces of the products after a series of polymerization time (10, 30, 60, 90, 120 min) (Table 2, entry 1). Source data for Fig. 3b is available (Supplementary Data 1).



their mixture (Supplementary Fig. 3d) revealed a decrease in the absorption derived from the N–H stretching vibration at approximately 3300 cm^{-1} from their mixture, although the absorption derived from the C=O stretching vibration at 1720 cm^{-1} remained unchanged. If one of the NH protons in U(4CF₃) is abstracted by TMGN, the absorption attributed to the C=O stretching vibration should disappear or decrease. Hence, the steric hindrance of TMGN around basic sites likely discourages proton abstraction even from relatively acidic U(4CF₃). Furthermore, the IR spectra of the mixture of I₃, U(4CF₃), and TMGN (Supplementary Fig. 3e) were almost identical to those of the mixture of U(4CF₃) and TMGN (Supplementary Fig. 3d). This is consistent with the hypothesized left-biased equilibrium in Fig. 4d. Although the equilibrium should be biased to the left, it is difficult to show the existence of propagating species on the right side of the equilibrium; the fact that the unitary ROP by TMGN did not proceed and that the BOROP by using TMGN and U(4CF₃) did is one of the results supporting the existence of the hypothesized equilibrium.

Fabrication of a highly transparent, elastic, and stretchy elastomer enabled by precisely-defined star-shaped PDMS

The established BOROP provides unexampled opportunities for various silicone-based materials. To ensure the feasibility of the study, we examined the potential application of our star-shaped PDMSs enabled by BOROP for silicone potting compounds (SPCs). SPCs are an important class of curable

liquid polysiloxanes used, for example, in electronics, medical applications, and microfluidics. Silicone elastomers can be formed simply by mixing two liquid polysiloxanes. To test the applicability of our chemistry to SPC, we synthesized a series of 3-armed star-shaped PDMSs with hydrosilane (\mathbf{P}_{H} : $\mathbf{P}_{\text{H}(10\text{k})}$, $\mathbf{P}_{\text{H}(25\text{k})}$, and $\mathbf{P}_{\text{H}(27\text{k})}$) and vinyl end groups (\mathbf{P}_{V} : $\mathbf{P}_{\text{V}(10\text{k})}$, and $\mathbf{P}_{\text{V}(25\text{k})}$) based on the developed BOROP of D3 (Supplementary Table 1). The BOROP conditions were controlled to have MWs of approximately 10 kDa and 25 kDa, and these MWs were adjusted to be distinctly lower or slightly higher than the critical entanglement MW (M_e) of PDMS (24.5 kDa)³², thus these conditions are suitable for examining the effect of MW and entanglement on mechanical properties. The synthesized \mathbf{P}_{H} s and \mathbf{P}_{V} s were then mixed in the presence of Karstedt's catalyst so that the hydrosilane and vinyl end groups of \mathbf{P}_{H} s and \mathbf{P}_{V} s, respectively, were equimolar, and their behavior as SPCs was examined (Fig. 5a). Moreover, to examine the effect of \bar{D} on the mechanical properties, industrial-grade PDMS with vinyl end groups and a broad \bar{D} ($\mathbf{P}_{\text{V}(S-7)}$) produced by equilibrium polymerization, such that the relationship between the branching point and the number of end groups is equivalent to that of 3-armed star-shaped PDMS, was also coupled to \mathbf{P}_{H} s to investigate its behavior as an SPC. Eventually, we fabricated a total of 5 silicon elastomers (\mathbf{S}_{E} : $\mathbf{S}_{\text{E}(10\text{k},10\text{k})}$, $\mathbf{S}_{\text{E}(10\text{k},\text{VS-7})}$, $\mathbf{S}_{\text{E}(25\text{k},25\text{k})}$, $\mathbf{S}_{\text{E}(27\text{k},10\text{k})}$, and $\mathbf{S}_{\text{E}(10\text{k},\text{VS-7})}$) from a series of \mathbf{P}_{H} s and \mathbf{P}_{V} s. According to the established protocol^{33,34}, we first evaluated the degree of crosslinking based on IR spectroscopy by the change in the absorbance derived from the Si–H bending vibration. It is clear from the comparison of IR spectra between $\mathbf{P}_{\text{V}(10\text{k})}$ (Supplementary Fig. 4a) and $\mathbf{P}_{\text{H}(10\text{k})}$ (Supplementary Fig. 4b) that the absorption derived from the Si–H group at 912 cm^{-1} is distinguishable from the other absorptions, and the Si–H absorption also appeared in the mixture of $\mathbf{P}_{\text{V}(10\text{k})}$ and $\mathbf{P}_{\text{H}(10\text{k})}$ (Supplementary Fig. 4c). In contrast, the Si–H absorption band disappeared from the IR spectrum of $\mathbf{S}_{\text{E}(10\text{k},10\text{k})}$ (Supplementary Fig. 4d), indicating the quantitative conversion of the hydrosilane end groups of $\mathbf{P}_{\text{H}(10\text{k})}$. This spectral change is more evident from the comparison of their magnified spectra (Supplementary Fig. 4e). Moreover, the disappearance of Si–H absorption was commonly observed in the spectra of $\mathbf{S}_{\text{E}(25\text{k},25\text{k})}$ (Supplementary Fig. 5a), $\mathbf{S}_{\text{E}(27\text{k},10\text{k})}$ (Supplementary Fig. 5b), $\mathbf{S}_{\text{E}(10\text{k},\text{VS-7})}$ (Supplementary Fig. 5c), and $\mathbf{S}_{\text{E}(27\text{k},\text{VS-7})}$ (Supplementary Fig. 5d). All of these results suggest that the degree of crosslinking can be determined to be approximately 100% based on IR spectroscopy.

Next, the rheological properties upon curing a series of mixtures of \mathbf{P}_{H} s and \mathbf{P}_{V} s were investigated. The time-dependent plots of G' and G'' measured immediately after preparing a series of mixtures commonly showed a significant increase in G' after the induction period (Fig. 5b). After approximately 1500 s, G' reached equilibrium, and G' of the resulting \mathbf{S}_{E} s varied depending on the starting \mathbf{P}_{H} s and \mathbf{P}_{V} s. (Fig. 5b). The equilibrated G' reached after at least two hours (G'_e) was determined to be 28 kPa for

Table 2 | BOROP of D3 initiated from I₃ catalyzed by TBD with a series of cocatalysts^a

Entry	Cocatalyst	[I ₃] ₀ : [TBD] ₀ : [HBA] ₀ : [D3] ₀	Time (min)	Conv. (%) ^b	M_n^c	\bar{D}^d
1	U(Cy)	1:1.5:3:135	90	91	12000	1.31
2	U(Cy)	1:0.75:3:135	90	88	23400	1.16
3	U(Cy)	1:0.75:1.5:135	90	93	24700	1.42
4 ^e	U(1CF ₃)	1:0.75:3:135	135	75	28600	1.17
5 ^e	U(4CF ₃)	1:0.75:3:135	60	57	28200	1.07
6 ^e	U(4CF ₃)	1:1.5:3:135	120	> 99	35700	1.09
7	TU	1:1.5:3:135	120	44	12600	1.09
8	TU	1:0.75:3:135	120	26	7300	1.06

^aThe polymerizations were performed at 30 °C. [D3]₀ = 2.14 M. Calculated number average molecular weight at the full consumption of D3 was 30,000.

^bConversion determined by ¹H NMR.

^cNumber average molecular weight, determined by SEC with RI detector.

^dDispersity ($\bar{D} = M_w/M_n$), determined by SEC. SEC measurements were performed after terminating with benzoic acid.

^e[D3]₀ = 2.25 M.

$S_{E(10k,10k)}$ (Fig. 5b, black line), whereas the G_e' of $S_{E(10k,VS-7)}$ was approximately 120 kPa (Fig. 5b, blue line), despite the M_n s of the starting $P_{V(10k)}$ and P_{VS-7} being essentially equivalent (Supplementary Table 1). As the \mathcal{D} of P_{VS-7} is broad (Supplementary Table 1, entry 6), the improvement in G_e' with P_{VS-7} could be explained by the occurrence of entanglement owing to the presence of long polymer chains. Moreover, $S_{E(25k,25k)}$ had the highest G_e' (Fig. 5b, red line) among the tested combinations of P_{HS} and P_{VS} (Supplementary Table 2, entry 3). Apparently, both $P_{H(25k)}$ and $P_{V(25k)}$ have MWs higher than M_e (Supplementary Table 1, codes 2 and 5), thus suggesting the effective formation of entanglement between polymer chains within the network. To verify the effect of entanglement, we next compared the rheological properties of the combination of $P_{H(27k)}$ and $P_{V(10k)}$. In this case, G_e' significantly decreased to 27 kPa (Supplementary Table 2, entry 4). If only the effect of MW on the mechanical properties is considered, G_e' should increase with decreasing MW of the precursors, i.e., with decreasing

network size, and the present decrease in G_e' is presumably due to the decrease in entanglement. On the other hand, the combination of $P_{H(27k)}$ and P_{VS-7} resulted in a decrease in G_e' to 33 kPa (Supplementary Table 2, entry 5), even though P_{VS-7} was expected to undergo entanglement. Although the details are not clear, the greater G_e' with $P_{H(10k)}$ (Supplementary Table 2, entry 2) than with $P_{H(27k)}$ (Supplementary Table 2, entry 5) may be due to the smaller network size. In any case, eliminating the effect of either MW or entanglement is difficult, and discussing their effects on physical properties separately is difficult. In contrast, it should be noted that these effects can be discussed separately with PDMSs with narrow \mathcal{D} .

Finally, the elastic nature of $S_{E(25k,25k)}$ was examined based on static mechanical analysis. Thus, a tensile test was conducted on $S_{E(25k,25k)}$, and the tensile modulus (E), elongation at break (ϵ_B), tensile strength (σ_T), and fracture energy (I) were determined to be 0.41 MPa, 330%, 0.48 MPa, and $1.2 \times 10^4 \text{ J m}^{-2}$, respectively, from the stress-strain curve (Fig. 5c). It would be meaningful to compare the mechanical properties of $S_{E(25k,25k)}$ with those of existing SPCs. Notably, the measured I ($1.2 \times 10^4 \text{ J m}^{-2}$) of our $S_{E(25k,25k)}$ was 10 to 100 times greater than those of silicone elastomers formed from widely used SPCs such as Sylgard 184 and was comparable to or higher than those of conventional PDMS composites ($I \sim 10^3\text{--}10^4 \text{ J m}^{-2}$)³⁵, despite our $S_{E(25k,25k)}$ did not contain any filler. Another intriguing property is its highly stretchy nature. While several studies indicate that the ϵ_B of silicone elastomers formed from Sylgard 184 reach 200%^{36,37}, $S_{E(25k,25k)}$ showed ϵ_B of 330%, demonstrating its highly stretchy nature. A more uniform network from the SPC would avoid stress concentrations at junction points, which likely resulted in the formation of highly stretchy elastomers with excellent mechanical properties.

Table 3 | ROP of D3 initiated from I_3 catalyzed by various organic bases with U(4CF₃)^a

Entry	Cat.	[I_3] ₀ : [Cat.] ₀ : [HBA] ₀ : [M] ₀	Time (min)	Conv. (%) ^b	M_n^c	\mathcal{D}^d
1	DMAP	1:1.5:3:135	120	N.D.		
2	DMAN	1:1.5:3:135	120	N.D.		
3	TMGN	1:1.5:3:135	120	26	6700	1.06
4	TMGN	1:1.5:3:135	360	80	13,000	1.10
5 ^e	TMGN	1:1.5:3:135	360	N.D.		

^aThe polymerizations were performed at 30 °C. [M]₀ = 2.4 M. Calculated number average molecular weight at the full consumption of D3 was 30,000.

^bConversion determined by ¹H NMR.

^cNumber average molecular weight, determined by SEC with RI detector.

^dDispersity ($\mathcal{D} = M_w/M_n$), determined by SEC. SEC measurements were performed after terminating with benzoic acid.

^eU(Cy) was used instead of U(4CF₃).

Fig. 4 | Binary organocatalytic ROP for the synthesis of star-shaped PDMSs. **a** Plots of conversion and \mathcal{D} against time and **(b)** SEC traces of the products after a series of polymerization time (60, 90, 120, 240, 360 min) (Table 3, entry 4). **c** Neutral and imidate-mediated H-bonding mechanisms for base and urea cocatalyzed ROP reported in the literature³⁶. **d** Proposed activation–deactivation mechanism for the present synergistic BOROP catalysis with TMGN and urea. Source data for Fig. 4a is available (Supplementary Data 1).

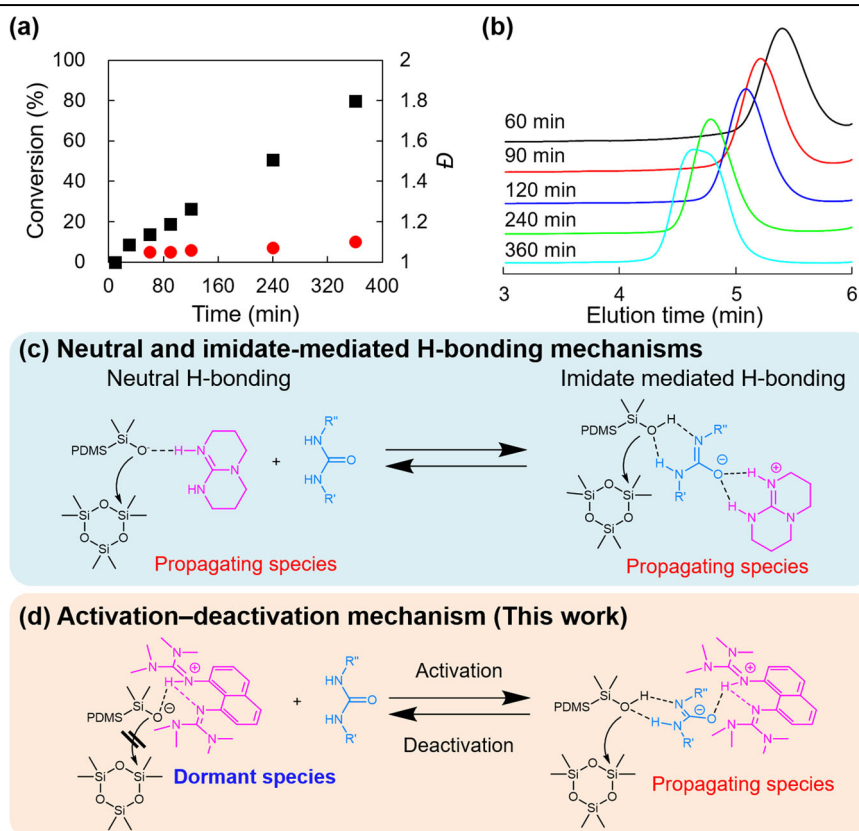
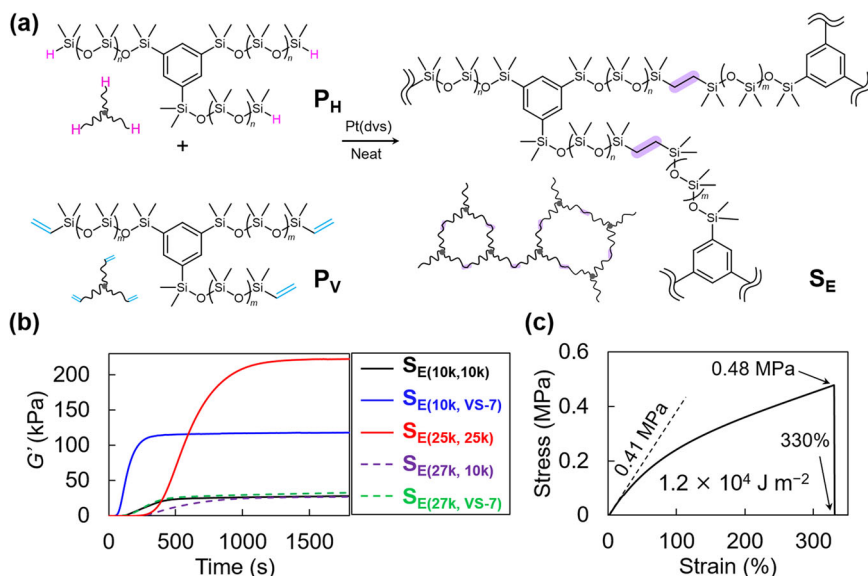


Fig. 5 | Formation of silicone elastomers from star-shaped PDMSs synthesized by the present BOROP. **a** Fabrication of silicone elastomer (S_E) by hydrosilylation reaction between P_H and P_V . **b** Time-course plots of G' and G'' during the formation of S_E (black line, $S_{E(10k, 10k)}$; blue line, $S_{E(10k, VS-7)}$; red line, $S_{E(25k, 25k)}$; purple dashed line, $S_{E(27k, 10k)}$; green dashed line, $S_{E(27k, VS-7)}$). **c** Stress–strain curve of $S_{E(25k, 25k)}$.



high monomer conversion. The BOROP developed here is also expected to benefit the development of various silicone-based materials after further studies on the effects of solvents³⁸ and other factors. To the best of our knowledge, the control of ROP using activation–deactivation equilibrium based on the properties of proton sponges is conceptually new. Moreover, star-shaped PDMSs synthesized by the established BOROP system were applied to SPCs, demonstrating the formation of highly stretchy elastomers with excellent mechanical properties. The binary catalyst system developed here has the potential to be applied to various ring monomers and will open the door for applications requiring precision polymer synthesis, such as human-body-related applications.

Methods

Materials

D3 (98%, Aldrich), DMAP, DMAN, TBD (98%, Aldrich), and TMGN were first dissolved in superdehydrated stabilizer-free THF (99.5%, Wako) and then dried over MS4A for 24 h before use. Chlorodimethylsilane (98%, Aldrich), chlorodimethylvinylsilane (98%, Aldrich), platinum(0)–1,3-divinyltetramethyldisiloxane complex solution (Karstedt's catalyst) (Pt~2% in xylene, Aldrich) and other reagents were used as received. Industrial-grade PDMS with vinyl end groups and a broad \bar{D} synthesized by equilibrium polymerization, such that the relationship between the branching point and the number of end groups is equivalent to that of 3-armed star-shaped PDMS (VS-7; $M_n = 12,000$, Lot no. 309001), was generously supplied by Shin-Etsu Chemical Co., Ltd. Benzene-1,3,5-triyl-tris(dimethylsilanol) (I_3)²⁰ and (thio)ureas⁹ were synthesized according to previously reported procedures.

Unitary catalytic ring-opening polymerization

In a typical procedure, a mixture of I_3 (10 mg, 0.10 mmol for OH groups), D3 (1.0 g, 4.5 mmol), and THF (1.8 mL) was prepared in a vial. To this mixture, a THF solution (0.3 mL) of TBD (7 mg, 0.050 mmol) was added to initiate ROP and the resulting solution was stirred at room temperature (25 °C). Aliquots were taken from the mixture at given times and subjected to 1H NMR and SEC analyses to determine monomer conversion, M_n , and \bar{D} . Likewise, other bases (DMAP, DMAN, and TMGN) were employed.

Binary catalytic ring-opening polymerization

In a typical procedure, a mixture of U(Cy) (22 mg, 0.10 mmol), I_3 (10 mg, 0.10 mmol for OH groups), D3 (1.0 g, 4.5 mmol), and THF (1.8 mL) was prepared in a vial. To this mixture, a THF solution (0.3 mL) of TBD (7 mg,

0.050 mmol) was added to initiate ROP and the resulting solution was stirred at room temperature (25 °C). Aliquots were taken from the mixture at given times and subjected to 1H NMR and SEC analyses to determine monomer conversion, M_n , and \bar{D} . Likewise, other combinations of bases (DMAP, DMAN, TBD, and TMGN) and (thio)urea were employed.

Synthesis of P_H and P_V

In a typical procedure, a mixture of U(Cy) (654 mg, 3.0 mmol), I_3 (300 mg, 3.0 mmol for OH groups), D3 (30.0 g, 135 mmol), and THF (54 mL) was prepared in a flask. To this mixture, a THF solution (9 mL) of TBD (209 mg, 1.5 mmol) was added to initiate ROP, and the resulting solution was stirred at room temperature (25 °C). After 1 h, a THF solution (9 mL) of benzoic acid (3.7 g, 30 mmol) was added to terminate the polymerization, and the solution was stirred at room temperature (25 °C). After 3 h, the mixture was concentrated to dryness and washed with acetone to afford three-armed star-shaped PDMS with hydroxy end groups. The yield was 25.0 g, which was used for the following end-capping reaction without further purification. Thus, the resulting PDMS (20.0 g) was dissolved in THF (40 mL), pyridine (11.6 mL, 144 mmol), and chlorodimethylsilane (5.23 mL, 48 mmol) in this order, and the resulting mixture was stirred at room temperature. After 17 h, the mixture was poured into excess H_2O /hexane, and the aqueous layer was separated and extracted with hexane. The combined hexane phase was washed with water, dried over Na_2SO_4 , and concentrated to dryness. The residue was washed successively with MeOH and acetone and dried under reduced pressure to afford three-armed star-shaped PDMS with hydrosilane end groups ($P_{H(25k)}$) as a colorless oil. The yield was 16.7 g. 1H NMR (500 MHz, acetone- d_6 , δ): 0.07 (–SiO(CH $_3$) $_2$ –), 4.71 (–Si(CH $_3$) $_2$ H), 7.76 (s, ArH). Number-averaged MW (M_n) and dispersity ($\bar{D} = M_w/M_n$) measured by SEC calibrated with polystyrene standards; $M_n = 25000$, $\bar{D} = 1.16$.

Three-armed star-shaped PDMS with vinyl end groups ($P_{V(25k)}$) was synthesized from the remaining three-armed star-shaped PDMS with hydroxy end groups (5.0 g) by using chlorodimethylvinylsilane as an end-capping reagent instead of chlorodimethylsilane. The yield was 4.0 g. 1H NMR (500 MHz, acetone- d_6 , δ): 0.07 (–SiO(CH $_3$) $_2$ –), 5.72 (dd, –Si(CH $_3$) $_2$ CH = CH $_2$), 5.92 (dd, –Si(CH $_3$) $_2$ CH = CH $_2$), 6.13 (dd, –Si(CH $_3$) $_2$ CH = CH $_2$), 7.76 (s, ArH). M_n and \bar{D} measured by SEC calibrated with polystyrene standards; $M_n = 25000$, $\bar{D} = 1.15$.

Likewise, other 3-armed star-shaped PDMSs with hydrosilane and vinyl end groups ($P_{H(10k)}$, $P_{H(27k)}$, and $P_{V(10k)}$) were synthesized. For 1H NMR spectra of I_3 , $P_{H(27k)}$, and $P_{V(25k)}$, see Supplementary Data 2.

Elastomer formation

In a typical procedure, a weighed amount of $P_{V(25k)}$ (1.5 g) and $P_{H(25k)}$ (1.5 g) was first mixed in a vial. To this mixture, Karstedt's catalyst (10 μ L) was added to allow the formation of elastomer, and then the mixture was immediately poured into a polystyrene antistatic weighing dish. After 1 h, the solidified PDMS elastomer (S_E) with a thickness of 1 mm was peeled from the dish and cut with a dumbbell blade (No. 7) to form a dumbbell-shaped tensile test specimen (ISO 527-2:2012, Type 5B). A tensile test of the resulting specimen was conducted at least 2 h after specimen preparation. For rheological measurements, the elastomer formation was performed on a measurement stage of an Anton Paar MCR 102 rheometer.

Data availability

All data supporting the findings of this study are available within this article and its Supplementary Information file. Source Data for Figs. 2b, 3b, and 4a can be found in Supplementary Data 1. The Original 1H NMR spectra of the compounds obtained in this manuscript are available in Supplementary Data 2. The data are also available from the corresponding author upon reasonable request.

Received: 11 July 2023; Accepted: 5 March 2024;

Published online: 21 March 2024

References

- Kamber, N. E. et al. Organocatalytic ring-opening polymerization. *Chem. Rev.* **107**, 5813–5840 (2007).
- Nederberg, F., Connor, E. F., Möller, M., Glauser, T. & Hedrick, J. L. New paradigms for organic catalysts: the first organocatalytic living polymerization. *Angew. Chem. Int. Ed.* **40**, 2712–2715 (2001).
- Pratt, R. C., Lohmeijer, B. G. G., Long, D. A., Waymouth, R. M. & Hedrick, J. L. Triazabicyclodecene: a simple bifunctional organocatalyst for acyl transfer and ring-opening polymerization of cyclic esters. *J. Am. Chem. Soc.* **128**, 4556–4557 (2006).
- Lohmeijer, B. G. G. et al. Guanidine and amidine organocatalysts for ring-opening polymerization of cyclic esters. *Macromolecules* **39**, 8574–8583 (2006).
- Connor, E. F., Nyce, G. W., Myers, M., Möck, A. & Hedrick, J. L. First example of N-Heterocyclic Carbenes as catalysts for living polymerization: organocatalytic ring-opening polymerization of cyclic esters. *J. Am. Chem. Soc.* **124**, 914–915 (2002).
- Dove, A. P. et al. N-Heterocyclic carbenes: effective organic catalysts for living polymerization. *Polymer* **47**, 4018–4025 (2006).
- Zhang, L. et al. Phosphazene bases: a new category of organocatalysts for the living ring-opening polymerization of cyclic esters. *Macromolecules* **40**, 4154–4158 (2007).
- Liu, S., Ren, C., Zhao, N., Shen, Y. & Li, Z. Phosphazene bases as organocatalysts for ring-opening polymerization of cyclic esters. *Macromol. Rapid Commun.* **39**, 1800485 (2018).
- Lin, B. & Waymouth, R. M. Urea anions: simple, fast, and selective catalysts for ring-opening polymerizations. *J. Am. Chem. Soc.* **139**, 1645–1652 (2017).
- Zhang, X., Fevre, M., Jones, G. O. & Waymouth, R. M. Catalysis as an enabling science for sustainable polymers. *Chem. Rev.* **118**, 839–885 (2018).
- Ottou, W. N., Sardon, H., Mecerreyes, D., Vignolle, J. & Taton, D. Update and challenges in organo-mediated polymerization reactions. *Prog. Polym. Sci.* **56**, 64–115 (2016).
- Bossion, A. et al. Opportunities for organocatalysis in polymer synthesis via step-growth methods. *Prog. Polym. Sci.* **90**, 164–210 (2019).
- Eduok, U., Faye, O. & Szpunar, J. Recent developments and applications of protective silicone coatings: a review of PDMS functional materials. *Prog. Org. Coat.* **111**, 124–163 (2017).
- Kantor, S. W., Grubb, W. T. & Osthoff, R. C. The mechanism of the acid- and base-catalyzed equilibration of siloxanes. *J. Am. Chem. Soc.* **76**, 5190–5197 (1954).
- Chojnowski, J. & Wilczek, L. Mechanism of the polymerization of hexamethylcyclotrisiloxane (D3) in the presence of a strong protonic acid. *Makromol. Chem.* **180**, 117–130 (1979).
- Kazama, H., Tezuka, Y. & Imai, K. A new bifunctional initiator for the living polymerization of hexamethylcyclotrisiloxane. *Polym. Bull.* **21**, 31–37 (1989).
- Goff, J., Sulaiman, S. & Arkles, B. Applications of hybrid polymers generated from living anionic ring opening polymerization. *Molecules* **26**, 2755 (2021).
- Lohmeijer, B. G. G. et al. Organocatalytic living ring-opening polymerization of cyclic carbosiloxanes. *Org. Lett.* **8**, 4683–4686 (2006).
- Brown, H. A., Chang, Y. A. & Waymouth, R. M. Zwitterionic polymerization to generate high molecular weight cyclic poly(carbosiloxane). *J. Am. Chem. Soc.* **135**, 18738–18741 (2013).
- Oka, M., Takagi, H., Miyazawa, T., Waymouth, R. M. & Honda, S. Photocleavable regenerative network materials with exceptional and repeatable viscoelastic manipulability. *Adv. Sci.* **8**, 2101143 (2021).
- Shi, L. et al. Ring-opening polymerization of cyclic oligosiloxanes without producing cyclic oligomers. *Science* **381**, 1011–1014 (2023).
- Kaljurand, I. et al. Extension of the self-consistent spectrophotometric basicity scale in acetonitrile to a full span of 28 pKa units: unification of different basicity scales. *J. Org. Chem.* **70**, 1019–1028 (2005).
- Raab, V., Kipke, J., Gschwind, R. M. & Sundermeyer, J. 1,8-Bis(tetramethylguanidino)naphthalene (TMGN): a new, superbasic and kinetically active “Proton Sponge”. *Chem. Eur. J.* **8**, 1682–1693 (2002).
- Henkel AG & Co. KGaA. Application number: 18185931.5. EU patent EP 3,599,256 B1 (2018).
- Fritz-Langhals, E. Unique superbases TBD (1,5,7-Triazabicyclo[4.4.0]dec-5-ene): from catalytic activity and one-pot synthesis to broader application in industrial chemistry. *Org. Process Res. Dev.* **26**, 3015–3023 (2022).
- Pothupitiya, J. U., Hewawasam, R. S. & Kiesewetter, M. K. Urea and Thiourea H-bond donating catalysts for ring-opening polymerization: mechanistic insights via (Non)linear free energy relationships. *Macromolecules* **51**, 3203–3211 (2018).
- Matyjaszewski, K. & Xia, J. Atom transfer radical polymerization. *Chem. Rev.* **101**, 2921–2990 (2001).
- Chandrasekhar, V., Boomishankar, R. & Nagendran, S. Recent developments in the synthesis and structure of Organosilanols. *Chem. Rev.* **104**, 5847–5910 (2004).
- Kannengießer, J.-F. et al. Synthesis and hydrogen-bond patterns of aryl-group substituted silanediols and -trials from alkoxy- and Chlorosilanes. *Chem. - Eur. J.* **27**, 16461–16476 (2021).
- Jakab, G., Tancon, C., Zhang, Z., Lippert, K. M. & Schreiner, P. R. Thio urea organocatalyst equilibrium acidities in DMSO. *Org. Lett.* **14**, 1724–1727 (2012).
- Xu, J. et al. Ionic H-bonding organocatalysts for the ring-opening polymerization of cyclic esters and cyclic carbonates. *Prog. Polym. Sci.* **125**, 101484 (2022).
- Yilgor, I., Eynur, T., Yilgor, E. & Wilkes, G. L. Contribution of soft segment entanglement on the tensile properties of silicone-urea copolymers with low hard segment contents. *Polymer* **50**, 4432–4437 (2009).
- Esteves, A. C. C. et al. Influence of cross-linker concentration on the cross-linking of PDMS and the network structures formed. *Polymer* **50**, 3955–3966 (2009).
- Nyczyk, A., Paluszkiwicz, C., Hasik, M., Cypryk, M. & Pospiech, P. Cross-linking of linear vinylpolysiloxanes by hydrosilylation – FTIR spectroscopic studies. *Vibrational Spectroscopy* **59**, 1–8 (2012).
- Chen, C., Fei, H.-F., Watkins, J. J. & Crosby, A. J. Soft double-network polydimethylsiloxane: fast healing of fracture toughness. *J. Mater. Chem. A* **10**, 11667–11675 (2022).
- Moučka, R., Sedláček, M., Osička, J. & Pata, V. Mechanical properties of bulk Sylgard 184 and its extension with silicone oil. *Sci. Rep.* **11**, 19090 (2021).

37. Wang, Z. et al. Stretchable materials of high toughness and low hysteresis. *Proc. Natl. Acad. Sci.* **116**, 5967–5972 (2019).
38. Fessler, W. A. & Juliano, P. C. Reactivity of solvated lithium n-Butyldimethylsilanolate with Organosiloxane substrates. *Product R&D* **11**, 407–410 (1972).

Acknowledgements

The authors are grateful to Dr. Minami Oka (The University of Tokyo) and Mr. Kazuki Fuke (The University of Tokyo) for their kind support for the synthesis of PDMSs. This work was supported by JSPS KAKENHI (Grant Numbers 21H01632 and 23K17337 S.H.), Fuji Seal Foundation (S.H.), and UTEC-UTokyo FSI Research Grant Program (S.H.).

Author contributions

S.H. conceived the concept of the project. H.O. performed the polymer synthesis and characterization. H.O., A.S. and S.H. performed elastomer formation and mechanical tests. S.H. wrote the paper, and S.H. supervised the project. All authors discussed the manuscript.

Competing interests

S.H. is an Editorial Board Member for *Communications Chemistry* but was not involved in the editorial review of, or the decision to publish this article. The authors declare no competing interests.

Additional information

Supplementary information The online version contains supplementary material available at <https://doi.org/10.1038/s42004-024-01140-3>.

Correspondence and requests for materials should be addressed to Satoshi Honda.

Peer review information *Communications Chemistry* thanks anonymous reviewer(s) for their contribution to the peer review of this work. A peer review file is available.

Reprints and permissions information is available at <http://www.nature.com/reprints>

Publisher's note Springer Nature remains neutral with regard to jurisdictional claims in published maps and institutional affiliations.

Open Access This article is licensed under a Creative Commons Attribution 4.0 International License, which permits use, sharing, adaptation, distribution and reproduction in any medium or format, as long as you give appropriate credit to the original author(s) and the source, provide a link to the Creative Commons licence, and indicate if changes were made. The images or other third party material in this article are included in the article's Creative Commons licence, unless indicated otherwise in a credit line to the material. If material is not included in the article's Creative Commons licence and your intended use is not permitted by statutory regulation or exceeds the permitted use, you will need to obtain permission directly from the copyright holder. To view a copy of this licence, visit <http://creativecommons.org/licenses/by/4.0/>.

© The Author(s) 2024